Data Extraction with ^{3}He detectors

P. Skensved and B.C. Robertson
SNO-STR-91-27

19-June-1991

Introduction

In [1] and [2] we have looked at the performance of the SNO detector with the 'default' neutral current detection option (NaCl dissolved in the D_2O). Three different Δm^2, $\sin^2 2\theta$ scenarios and the case of vacuum oscillations were investigated. Data were generated to simulate a 3 year experiment : a light water fill, a heavy water fill and finally a heavy water plus NaCl fill.

In this paper we will compare a similar 3 year experiment for a SNO detector which uses ^{3}He proportional counters to detect the neutrons created by the Neutral Current reaction.

Calculations

The standard Monte Carlo code [1-5] was modified to include 109 cylindrical tubes mounted vertically on a 99 cm spacing grid in the D_2O. The tubes were assumed to have an outside diameter of 5 cm, to have a refractive index of 4.0 and to be highly absorbing to photons with a wavelength between

300 and 700 nm. A material with a refractive index of 4.0 would reflect 25% at normal incidence when immersed in water. The present design calls for thin acrylic tubes coated with a metal on the inside. Such tubes would likely have a lower refractive index so the calculation probably represents a 'worst case scenario'.

Energy calibration/resolution and reconstruction effects

Two questions immediately come to mind when one introduces the idea of ^{3}He counters in the D_2O : how much light is lost and will the tubes destroy the spherical symmetry ? Figure 1a shows the reconstructed energy for ten thousand 10.511 MeV electrons started uniformly throughout the D_2O for the standard SNO detector. Figure 1b shows the same with the ^{3}He counters present. We clearly lose both light and resolution. The number of hits per MeV goes from 9.5 to 8.1 but the width of the distribution stays the same, meaning that the percentage resolution gets worse.

To test directional effects simulations were done for the ^{3}He tube configuration with 10.511 MeV electrons started near the center of the D_2O in three different directions : along the z-axis, in the x-y plane 45° to the x-axis and along the x-axis (figures 2 to 4). There is little difference in either the cosine of the angle between the electron and the reconstructed direction and in the reconstructed energy (table 1).

Backgrounds

As in [1] we use the 'White Book' [6] radioactivity levels for the detector components (table 2) with the added assumption that the major radioactivity in the ^{3}He counters is the acrylic tubing (1/8 inch wall thickness). If we take the 'White Book' numbers for acrylic then the 109 counter contribute a little more than 10% of the D_2O in terms of neutrons. This is comparable to the contribution from the NaCl in the default option. For simplicity we have therefore used the same neutron production numbers for the ^3He tubes as were used for the NaCl in [1]. Based on these and a production rate from the sun of 4500 neutrons per year [1] we arrive at table 3.

Extraction of data

Figure 5 shows a summary of signals and backgrounds (per year) reconstructed inside a radius of 600 cm assuming vacuum oscillations and a total flux of 5.8×10^6 cm^2 s^{-1}. This is to be compared with figure 1 in [1] (reproduced here as figure 6). The threshold is somewhat higher but the smaller Neutral Current (Čerenkov) signal helps in sorting out the different components.

For the analysis we follow the same procedure as in [1] where the data was sorted according to angle and energy (40×200 bins) and the angular projections were fitted with the elastic scattering angular distribution plus a term of form $1 - \frac{1}{3} \times \cos\theta$ plus a constant (representing the sum of the Neutral Current part and the background). In contrast with [1] year 2 and 3 has the detector in the same configuration and consequently we just sum the two. The analysis is done for an outer radius of 600 cm only.

Some typical fits to the sum of years 2 and 3 are shown in figures 7b to 7e as a function of lower threshold. Figure 7a is the corresponding energy projection for all values of the angle. At 40 hits we include a sizable background which decreases very fast with increasing threshold. However at high N_{hit} there is not much of an ES signal left. Fits for a fixed threshold of $N_{hit} = 50$ are displayed in figures 8 to 11 for vacuum oscillations, $\Delta m^2 = 10^{-6}$, 10^{-5} and 10^{-4} for year 1 and years 2 + 3.

The fits are summarized in tables 4 and 5 where we list the lower threshold, the fitted values and the Monte Carlo input numbers plus the total χ^2. The same numbers are presented in ratio form in table 6. At around $N_{hit} = 50$ we more or less extract what is put in.

Expected rates per year, based on the high statistics multiyear runs, are listed in table 7 where we also include the expected number from the

^{3}He counters. We assume an efficiency of 85% for these.

Ratios of extracted signals to that expected from the standard solar model are summarized in table 8. The NC flux listed is that determined from the capture in the deuterium not the one determined from the ^{3}He counters. Due to the poor statistics and the high correlation with the CC spectrum these numbers are virtually meaningless. The other ratios track very well and if the uncertainty in doing the subtraction of the neutron background in the ^{3}He counters is low enough (overall uncertainty less than about 15 %) then we could prove the presence of oscillations for any of the 4 cases studied at the 3σ level.

Another way of analyzing the data is to form the ratio of combinations of sums and differences of the total number of counts above some threshold similarly to what was done in [1].This assumes constant fluxes and constant backgrounds as a function of time. If T_i is the total number of counts in year i and H is the average number of counts in the ^{3}He counters then the ratio $r = \frac{H}{T_3 - T_2 - 2 \times T_1}$ is related to $R' = H_{obs}/CC_{obs}$ by $R' = \frac{r}{1 - n \times r}$ where n is the ratio of the neutron detection efficiencies for deuterium and ^{3}He. It can be determined accurately with a source.

Figure 12 shows

$$R = [H_{obs}/CC_{obs}] \times [CC_{mc}/H_{mc}]$$

where CC_{mc} is evaluated based on the no oscillation scenario for a lower threshold on $N_{hit} = 50$ plotted as function of the neutron background in units of 965 detected in the ^{3}He counters per year. This is the 'White Book' prediction; however it does not include any α background in the ^{3}He detectors. As in [1] we assume a 20% uncertainty in determining the total neutron background. The uncertainty in H_{obs} is just the statistical one. There is a small improvement over the equivalent figure for NaCl figure 13 (figure 11 from [1]). In both cases we have assumed fluxes which do not vary as a function of time. The reason why we get approximately the same answer is that the correlation between the charged current and the neutral current components is essentially zero when one does subtractions. Simultaneous fit of CC and NC on the other hand introduces a large correlation coefficient which increases the uncertainty significantly.

Conclusions

We have shown that the ^{3}He tubes do not interfere significantly with the Čerenkov light and that it is still possible to get a reasonable signal from the CC and ES reactions. The amplitude of the ES signal can be extracted over a wide range of MSW parameters from the angular fits alone as can the CC signals. In terms of answering the question of whether any of the four chosen scenarios differ from the no oscillation case by more than 3σ the ^{3}He option is doing a little better than NaCl with straight subtraction. In both cases we have assumed that the total neutron background could be determined by other means to 20% but we have not specifically included α-backgrounds or any other systematic uncertainties in the ^{3}He counters.

References

[1] SNO-STR-91-06

[2] SNO-STR-91-28

[3] SNO-STR-89-01

[4] SNO-STR-89-43

[5] SNO-89-15

[6] SNO-87-12

e^- direction	Reconstructed N_{hit}	Reconstructed cos
(0,0,1)	87.3 (11.4)	.91 (.11)
$(\frac{1}{\sqrt{2}},\frac{1}{\sqrt{2}},0)$	84.1 (11.1)	.89 (.12)
(1,0,0)	84.0 (11.1)	.89 (.11)

Table 1: Average number of reconstructed hits and average cosine of angle between e^- direction and reconstructed direction. Numbers in brackets are second moments. A total of 1,000 electron showers (10.511 MeV total energy) were started at (50,0,0).

	Mass(tonnes)	Th(g/g)	U(g/g)
D_2O	1000	11×10^{-15}	11×10^{-15}
Acrylic	30.0	1.9×10^{-12}	3.6×10^{-12}
H_2O	1667.7	22×10^{-15}	15×10^{-15}
PMT	7.5	0.1×10^{-6}	0.1×10^{-6}

Table 2: Masses and levels of ^{232}Th and ^{238}U in various detector components

Component	Production rate per year	Captures per year ^{3}He	Captures per year deuterium
Sun	4500	2049	566
Int. background	1432	652	180
Ext. background	2535	483	127

Table 3: Neutron production rates and capture rates per year. Internal background refers to neutrons arising from the D_2O and the ^{3}He counters. The rest (acrylic vessel, H_2O, PMT's etc. is included in the external component

Δm^2/ $\sin^2 2\theta$	Thres. N_{hit}	ES Fit	ES M.C.	Background Fit	Background M.C.	χ^2 (40 pts.)
vac.	40	307 (25)	336	1137 (38)	1108	121.
	50	202 (15)	217	62 (10)	47	33.1
	60	123 (11)	123	5 (3)	5	38.2
	70	74 (9)	74	2 (2)	2	34.0
10^{-6} 0.01	40	546 (30)	575	1137 (38)	1108	114.
	50	360 (20)	375	62 (10)	47	29.1
	60	223 (15)	225	8 (4)	5	32.3
	70	132 (12)	133	3 (2)	2	36.3
10^{-5} 0.3	40	39 (16)	53	1122 (37)	1108	132.
	50	35 (7)	35	47 (8)	47	35.2
	60	22 (5)	21	4 (3)	5	35.6
	70	10 (3)	10	2 (2)	2	32.7
10^{-4} 0.01	40	155 (20)	175	1128 (37)	1108	130.
	50	73 (10)	82	56 (9)	47	27.4
	60	31 (6)	31	54 (3)	5	31.3
	70	13 (4)	13	3 (2)	2	35.6

Table 4: Year 1 data for $0 \leq r \leq 600$ cm. Angular distribution fitted to ES(θ) + constant.

Δm^2/	Thres.	ES		CC		Background + NC		χ^2
$\sin^2 2\theta$	N_{hit}	Fit	M.C.	Fit	M.C.	Fit	MC	(40 pts.)
	40	711 (59)	614	6708 (659)	5853	2207 (692)	2263 + 895	59.7
vac.	50	499 (43)	412	4535 (477)	4486	242 (497)	119 + 259	28.7
	60	295 (32)	251	2967 (374)	3043	86 (389)	12 +42	29.2
	70	126 (14)	141	1500 (285)	1854	374 (295)	3 + 2	47.6
	40	1104 (71)	1016	9205 (764)	8807	2673 (803)	2263 + 895	99.2
10^{-6}	50	741 (52)	647	7272 (581)	6815	-173 (605)	119 + 259	54.4
0.01	60	439 (40)	402	4789 (465)	4693	-79 (482)	12 + 42	48.0
	70	278 (29)	237	3476 (353)	2845	-667 (363)	3 + 2	36.4
	40	104 (37)	118	1450 (439)	1023	2745 (464)	2263 + 895	157.
10^{-5}	50	83 (20)	75	810 (229)	767	327 (240)	119 + 259	36.4
0.3	60	40 (14)	43	317 (159)	506	247 (166)	12 + 42	39.0
	70	20 (9)	26	228 (113)	285	68 (117)	3 + 2	42.8
	40	324 (46)	319	2922 (517)	2246	2694 (545)	2263 + 895	105.
10^{-4}	50	147 (23)	136	1066 (255)	1005	308 (267)	119 + 259	37.9
0.01	60	70 (13)	49	606 (143)	389	-182 (147)	12 + 42	39.7
	70	16 (7)	18	163 (80)	136	-18 (83)	3 + 2	41.1

Table 5: Year 2 + 3 data for $0 \leq r \leq 600$ cm. Angular distribution fitted to ES(θ) + [1 - $\frac{1}{3}$ cos θ] + constant.

Δm^2/ $\sin^2 2\theta$	Thres. N_{hit}	Year 1 ES	Year 2 + 3 ES	Year 2 + 3 CC	Year 2 + 3 B + NC
vac.	40	0.91 (.07)	1.16 (.10)	1.15 (.11)	0.70 (.22)
	50	0.93 (.07)	1.21 (.10)	1.01 (.11)	0.6 (1.0)
	60	1.00 (.09)	1.18 (.13)	0.98 (.12)	1.6 (7.2)
	70	1.00 (.12)	0.89 (.18)	0.81 (.15)	75. (59.)
10^{-6} .01	40	0.95 (.05)	1.09 (.07)	1.05 (.09)	0.85 (.25)
	50	0.96 (.05)	1.15 (.08)	1.07 (.09)	-0.5 (1.6)
	60	0.99 (.07)	1.09 (.10)	1.02 (.10)	-1.5 (8.9)
	70	0.99 (.09)	1.17 (.12)	1.22 (.12)	133. (71.)
10^{-5} 0.3	40	0.74 (.30)	0.96 (.31)	1.42 (.43)	0.87 (.15)
	50	1.00 (.20)	1.11 (.27)	1.06 (.30)	0.87 (.63)
	60	1.05 (.24)	0.93 (.33)	0.63 (.31)	4.6 (3.1)
	70	1.00 (.30)	0.77 (.35)	0.80 (.40)	14. (23.)
10^{-4} .01	40	0.89 (.11)	1.02 (.14)	1.30 (.23)	0.85 (.17)
	50	0.89 (.12)	1.08 (.17)	1.06 (.25)	0.81 (.71)
	60	1.00 (.19)	1.43 (.27)	1.56 (.37)	-3.4 (2.7)
	70	1.00 (.31)	0.89 (.39)	1.20 (.59)	-3.6 (17.)

Table 6: Ratios of fitted numbers to Monte Carlo input numbers for r $\leq$ 600 cm

Threshold		ES	CC	NC	
N_{hit}	E(MeV)			D_2O	^{3}He
40	4.9	1000	8683	285	1742
50	6.2	656	6594	89	1742
60	7.4	406	4464	13.7	1742
70	8.6	232	2653	1.04	1742

Table 7: Expected rates based on multiyear distributions inside r = 600 cm for Standard Solar Model with 5.8×10^6 ν_e per cm^2 per sec. The ^{3}He counters are assumed to have an efficiency of 85%.

Δm^2/ $\sin^2 2\theta$	Thres. N_{hit}	Year 1 ES	Year 2 + 3 ES	CC	NC
	40	.31 (.03)	.36 (.03)	.39 (.04)	3.9 (1.2)
vac.	50	.31 (.02)	.38 (.03)	.34 (.04)	1.4 (2.8)
	60	.30 (.03)	.36 (.04)	.33 (.04)	3.1 (14.)
	70	.32 (.04)	.27 (.03)	.28 (.05)	180. (142.)
	40	.55 (.03)	.55 (.04)	.53 (.04)	4.7 (1.4)
10^{-6}	50	.55 (.03)	.56 (.04)	.55 (.04)	-1.0 (3.4)
.01	60	.55 (.04)	.55 (.05)	.54 (.05)	-2.9 (18.)
	70	.57 (.05)	.60 (.06)	.66 (.07)	-321. (175.)
	40	.04 (.02)	.05 (.02)	.08 (.03)	4.8 (0.8)
10^{-5}	50	.05 (.01)	.06 (.02)	.06 (.02)	1.8 (1.3)
0.3	60	.05 (.01)	.05 (.02)	.04 (.02)	9.0 (6.1)
	70	.04 (.01)	.04 (.02)	.04 (.02)	33. (56.)
10^{-4}	40	.16 (.02)	.16 (.02)	.17 (.03)	4.7 (1.0)
.01	50	.11 (.02)	.11 (.02)	.08 (.02)	1.7 (1.5)
	60	.08 (.01)	.09 (.02)	.07 (.02)	-6.6 (5.4)
	70	.06 (.02)	.03 (.02)	.03 (.02)	-8.7 (40.)

Table 8: Ratios of fitted numbers to numbers expected from the Standard Solar Model with a ν_e flux of 5.8×10^6 cm^{-2} s^{-1} for r $\leq$ 600 cm

Figure 1a

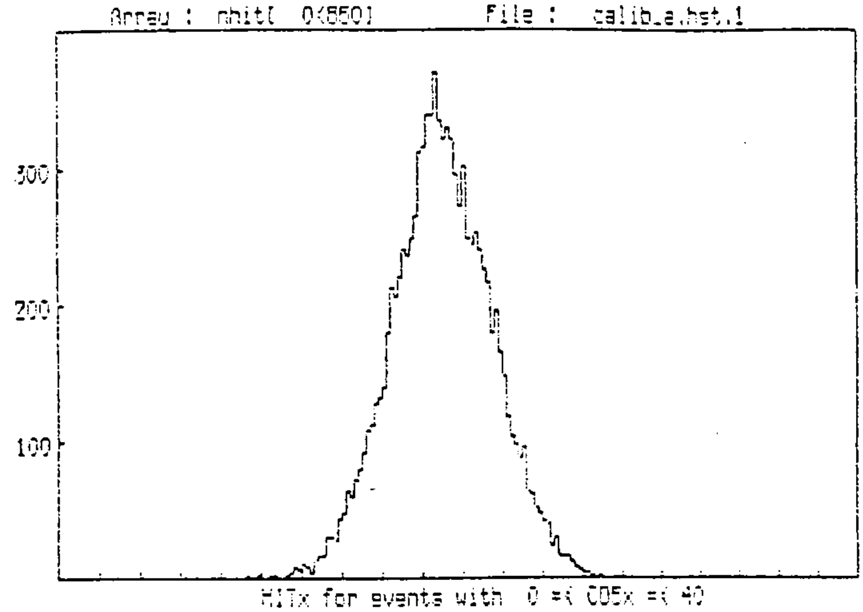
Array : nhit[0<650]
File : calib_a.hst.1
300
200
100
HITx for events with 0 =< COSx =< 40

1b

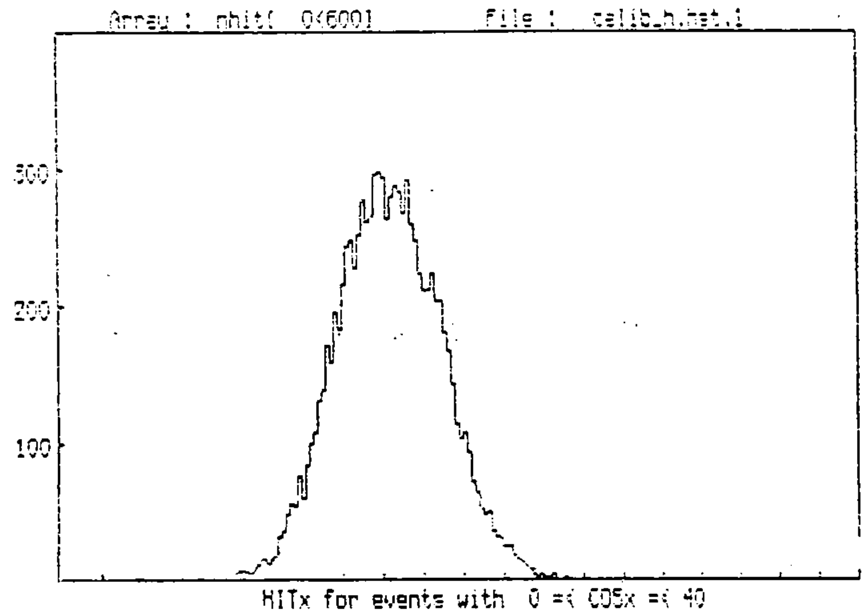
Array : nhit[0<600]
File : calib_h.hst.1
300
200
100
HITx for events with 0 =< COSx =< 40

Figure 2

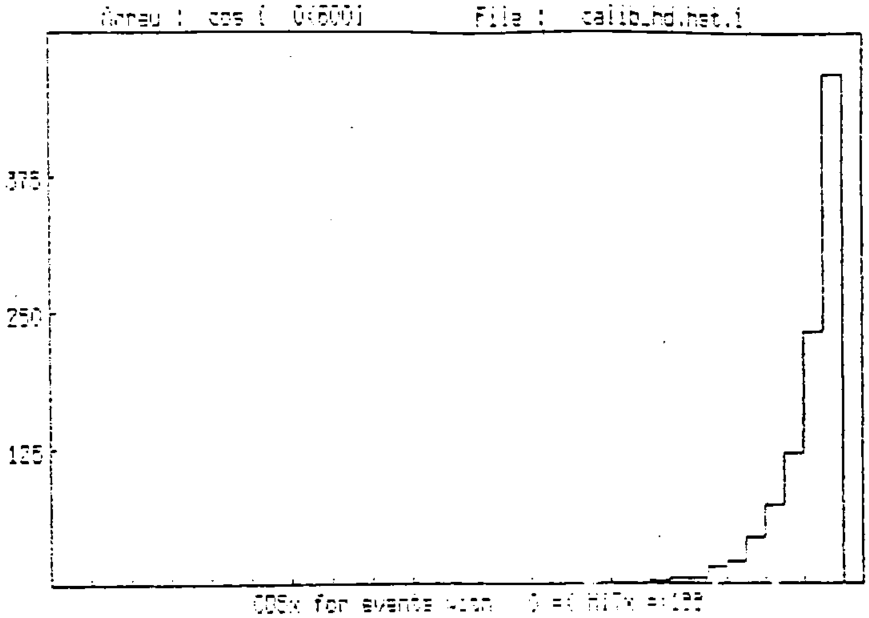
Array : cos (0:600) File : calib_hd.hst.1
375
250
125
COSx for events with

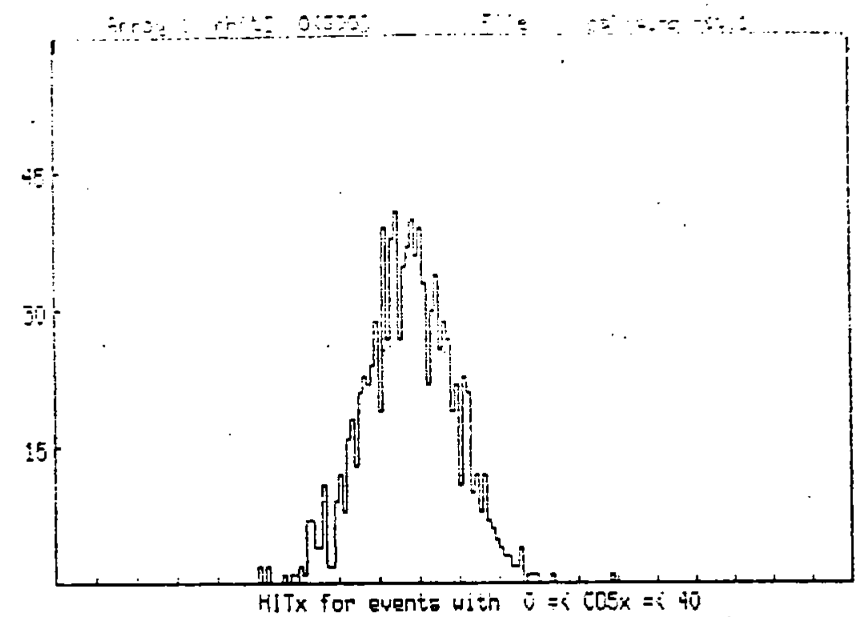
45
30
15
HITx for events with 0 =< COSx =< 40

Figure 3

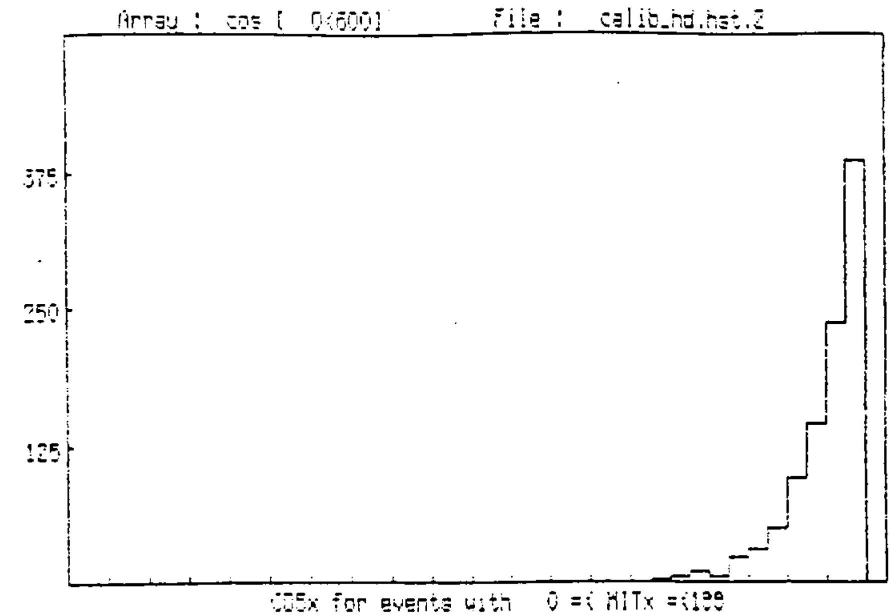

Array : cos [0(600)
File : calib_hd.hst.2
375
250
125
COSx for events with 0 =< HITx =<100

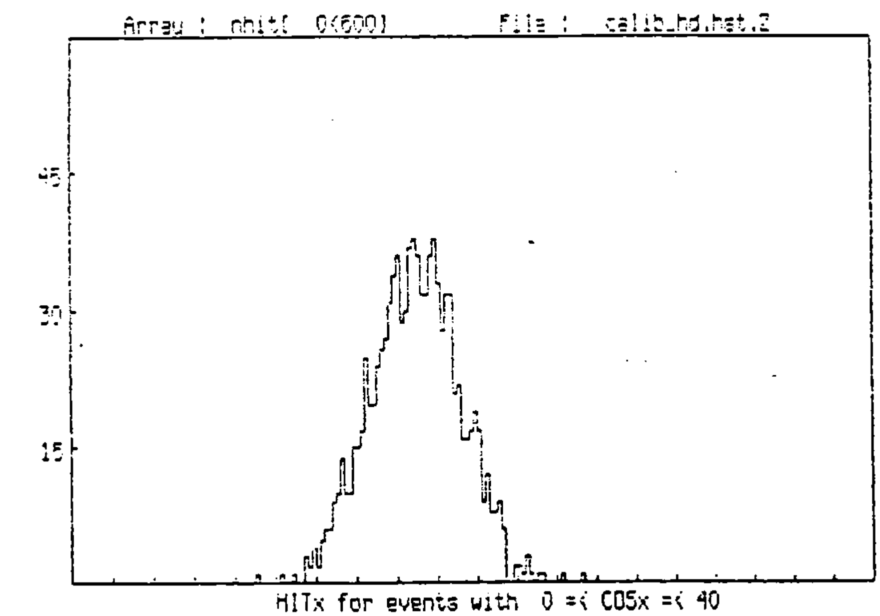

Array : nhit[0(600)
File : calib_hd.hst.2
45
30
15
HITx for events with 0 =< COSx =< 40

Figure 4

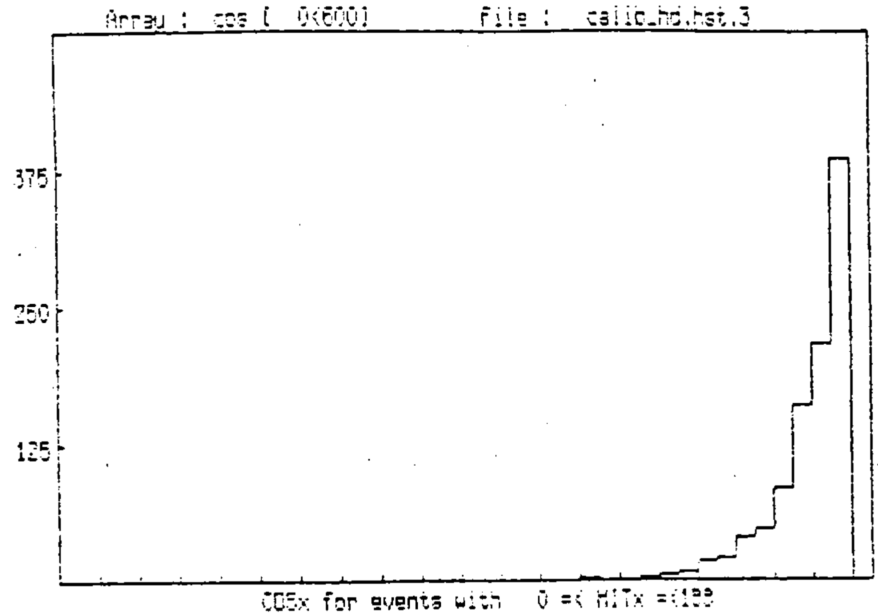

Array : cos [0(600]
File : calib_hd.hst.3
375
250
125
COSx for events with 0 =< HITx

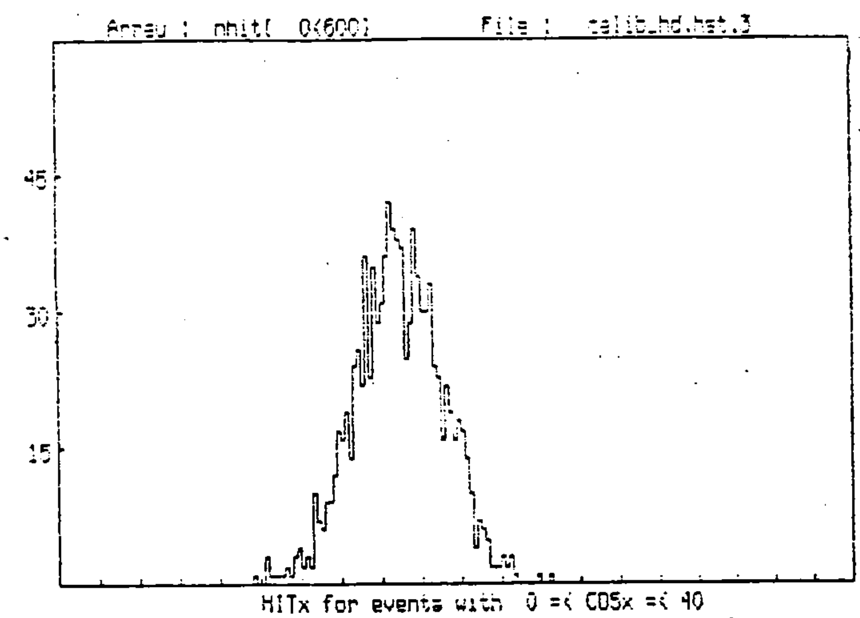

Array : nhit[0(600]
File : calib_hd.hst.3
45
30
15
HITx for events with 0 =< COSx =< 40

Figure 5

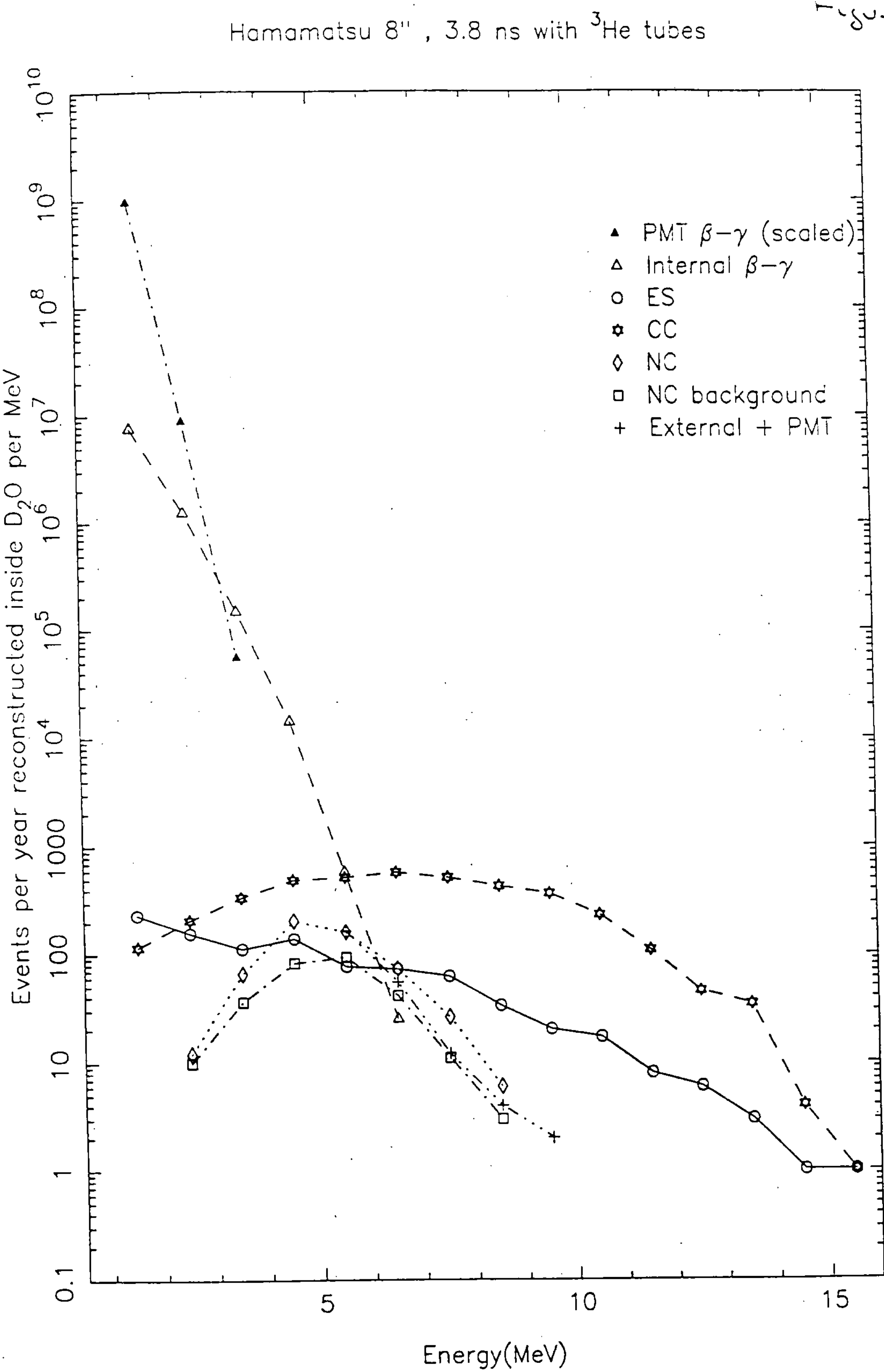

Hamamatsu 8'' , 3.8 ns with ^{3}He tubes
PMT $\beta-\gamma$ (scaled)
Internal $\beta-\gamma$
ES
CC
NC
NC background
External + PMT
Events per year reconstructed inside D_2O per MeV
Energy(MeV)
0.1
1
10
100
1000
10^4
10^5
10^6
10^7
10^8
10^9
10^{10}
5
10
15

Figure 6

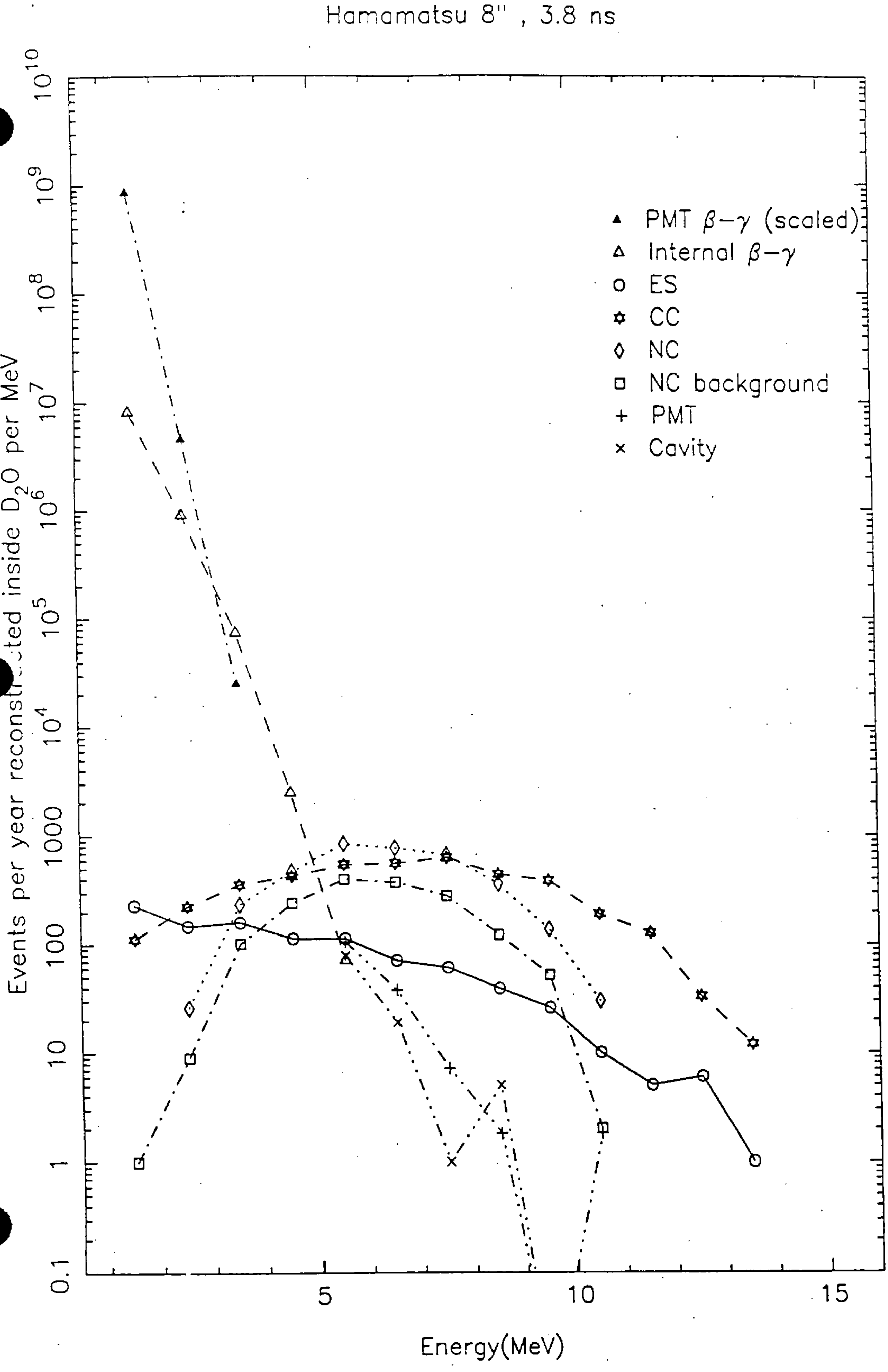

Hamamatsu 8", 3.8 ns
PMT β−γ (scaled)
Internal β−γ
ES
CC
NC
NC background
PMT
Cavity
Events per year reconstructed inside D2O per MeV
Energy(MeV)
0.1
1
10
100
1000
10^4
10^5
10^6
10^7
10^8
10^9
10^10
5
10
15

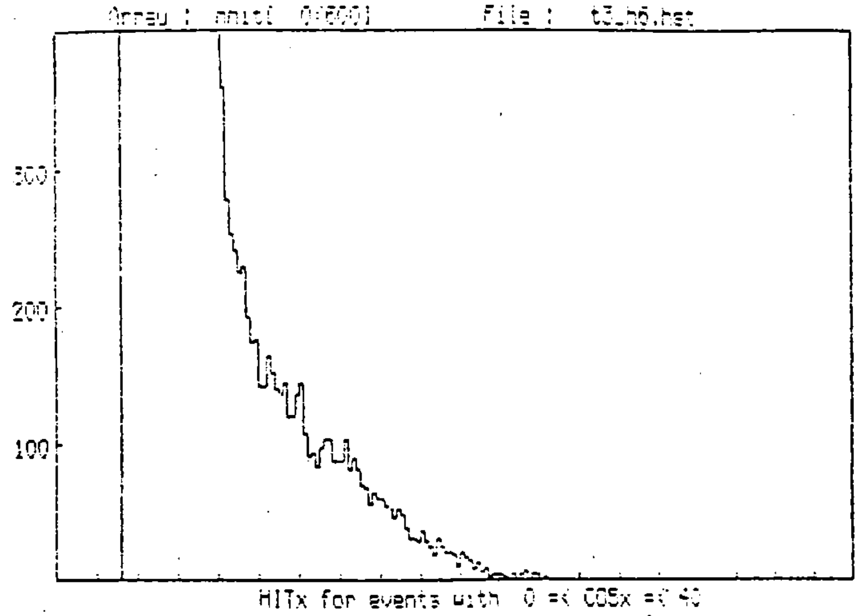

Figure 7a

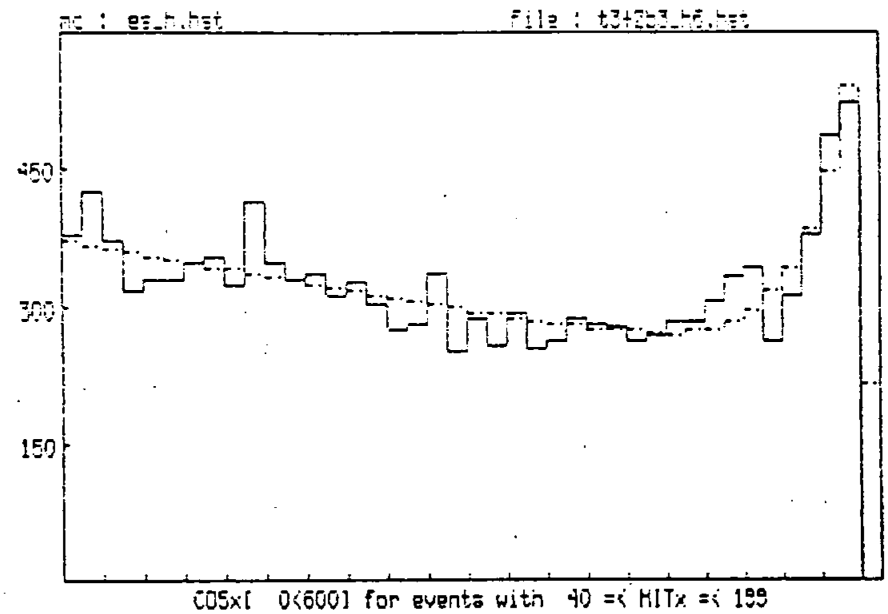

7b

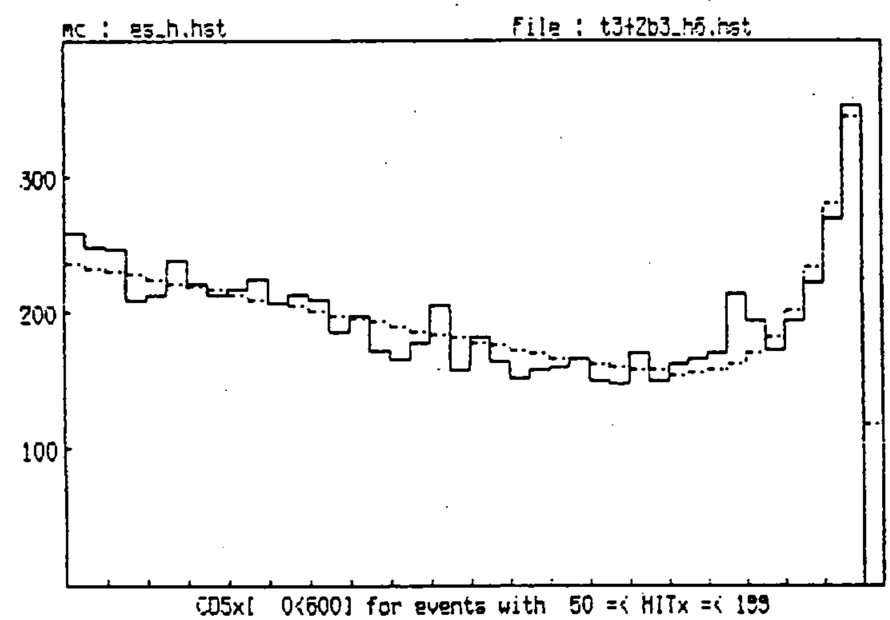

7c

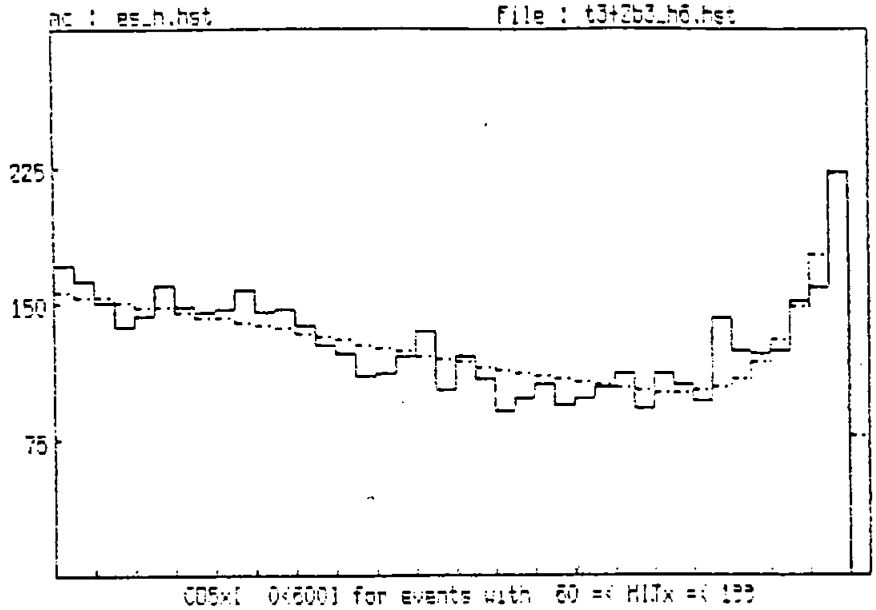
mc : es_h.hst
File : t3+2b3_h6.hst
225
150
75
CD5x[0<600] for events with 60 =< HITx =< 199

7d

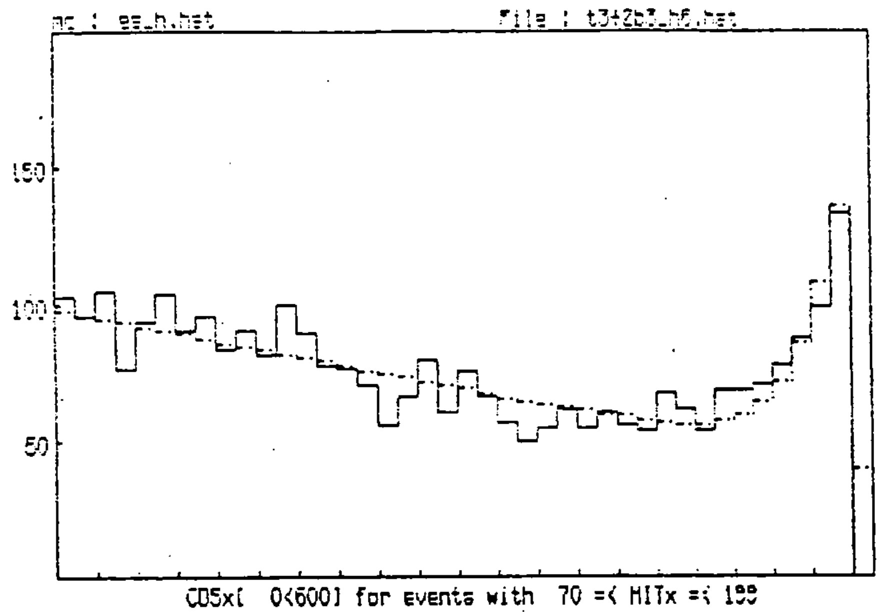
mc : es_h.hst
File : t3+2b3_h6.hst
150
100
50
CD5x[0<600] for events with 70 =< HITx =< 199

7e

Figure 8

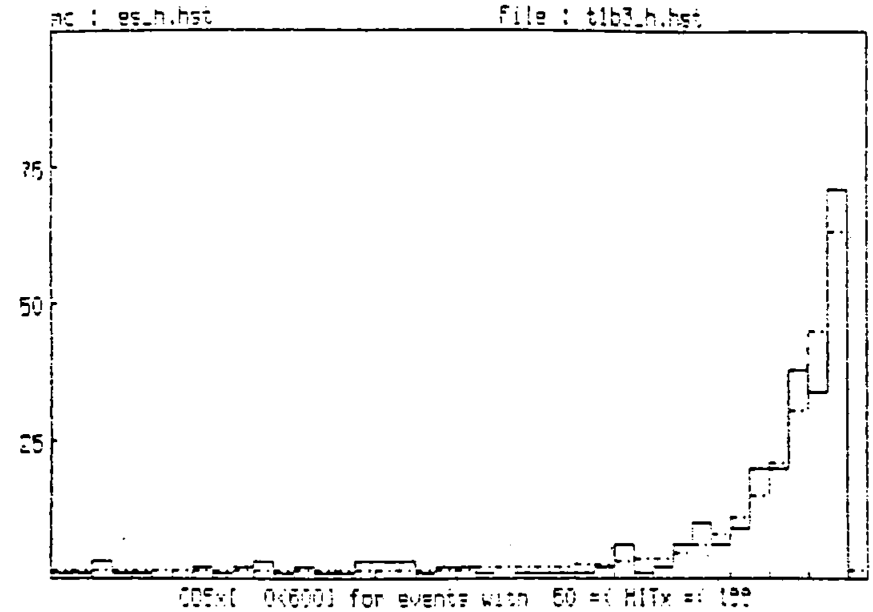

mc : es_h.hst
file : t1b3_h.hst
75
50
25
COSx[Q(600] for events with 50 =< HITx =< 199

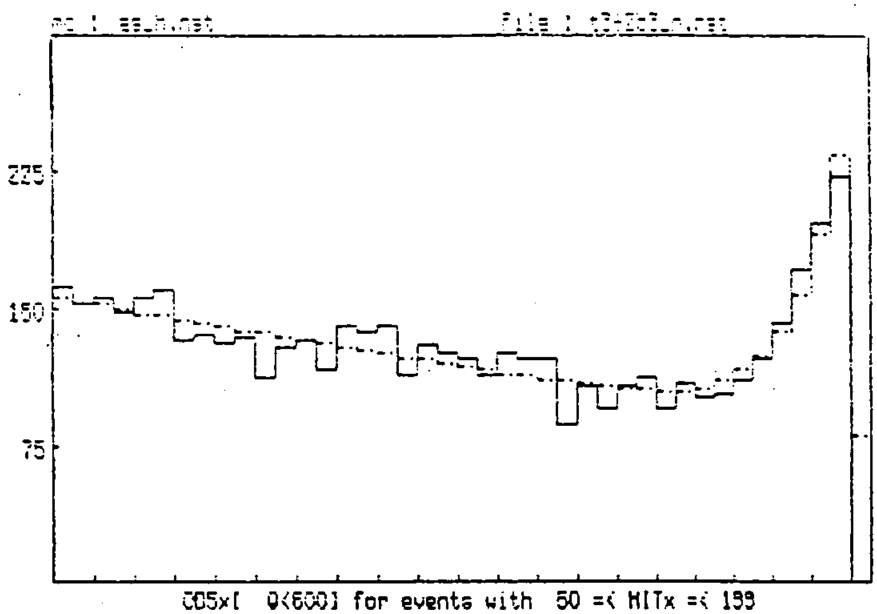

mc : es_h.hst
225
150
75
COSx[Q(600] for events with 50 =< HITx =< 199

Figure 9

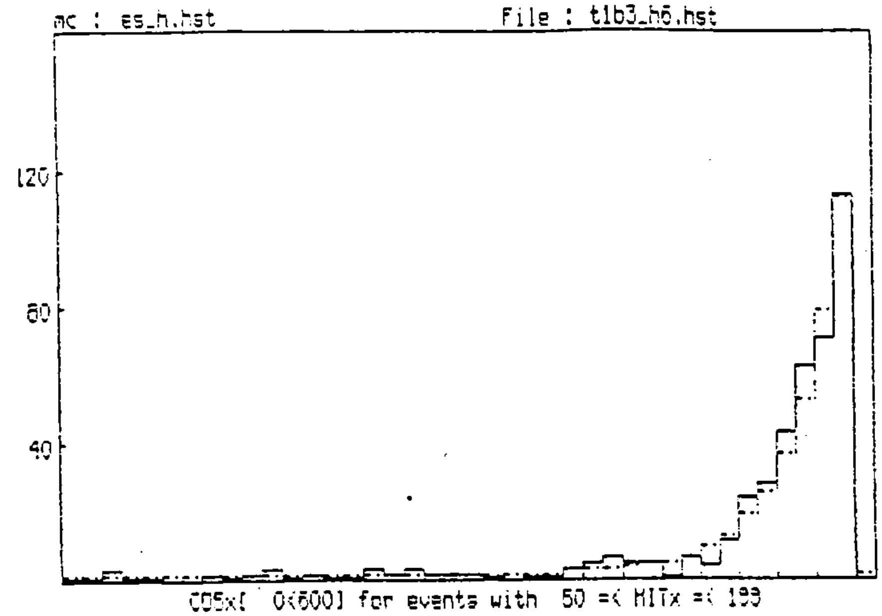

mc : es_h.hst
File : t1b3_h6.hst
120
80
40
C05x(0(600) for events with 50 =< HITx =< 199

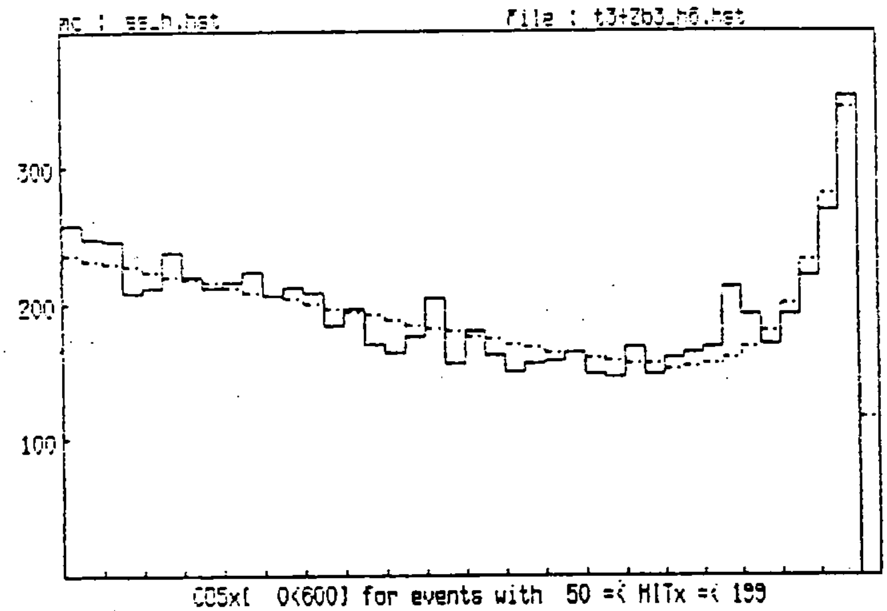

mc : es_h.hst
File : t3+2b3_h6.hst
300
200
100
C05x(0(600) for events with 50 =< HITx =< 199

Figure 10

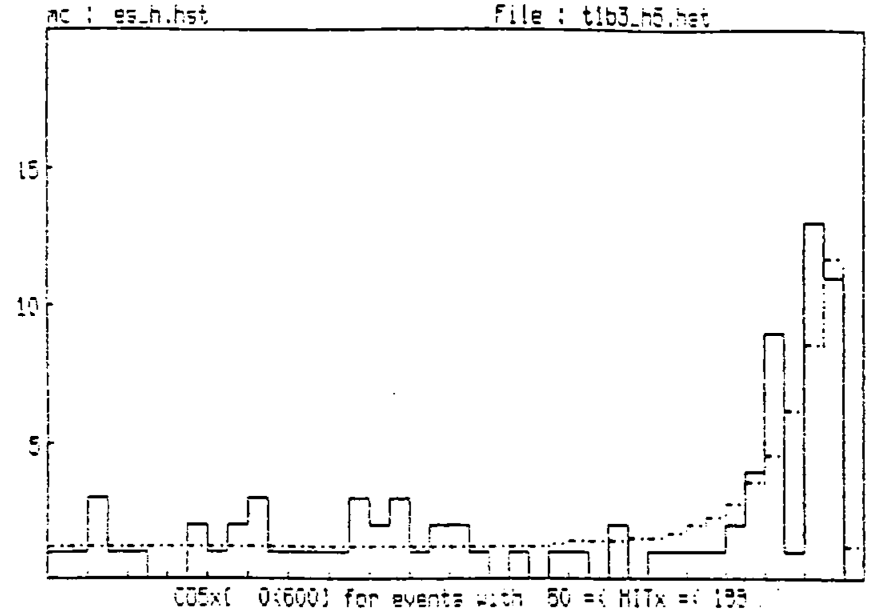
mc : es_h.hst
File : t1b3_h5.hst
15
10
5
C05x[0<600] for events with 50 =< HITx =< 199

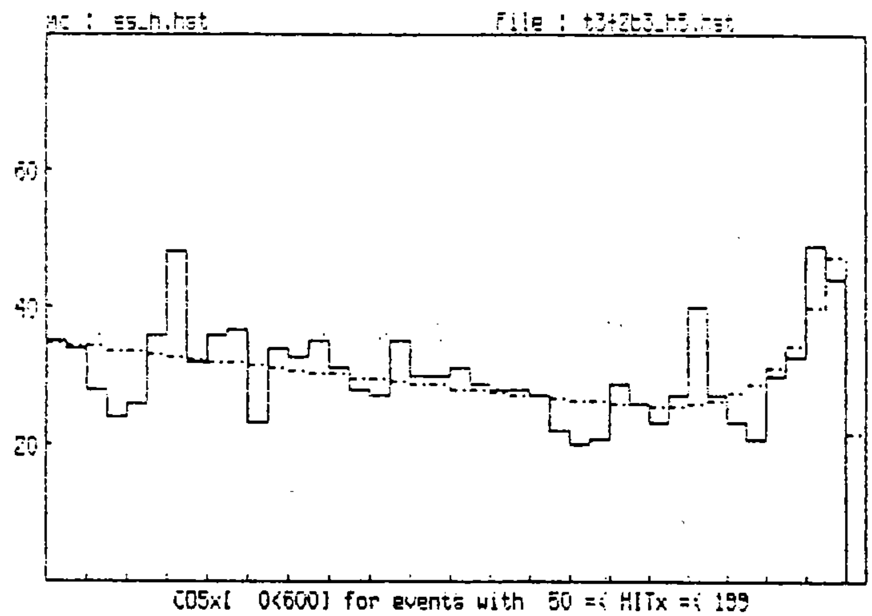
mc : es_h.hst
File : t3+2b3_h5.hst
60
40
20
C05x[0<600] for events with 50 =< HITx =< 199

Figure 11

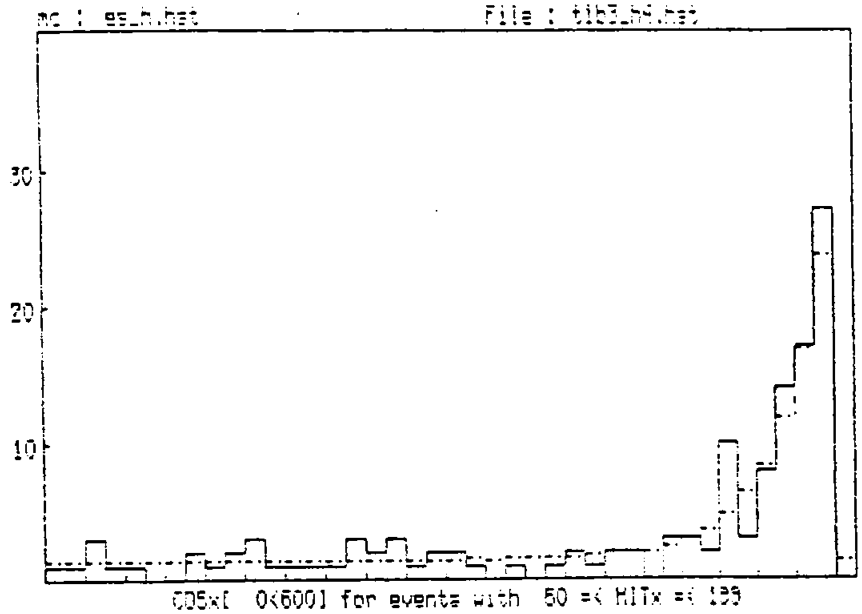

mc : es_h.hst
File : t1b3_h4.hst
30
20
10
CD5x[0<600] for events with 50 =< HITx =< 199

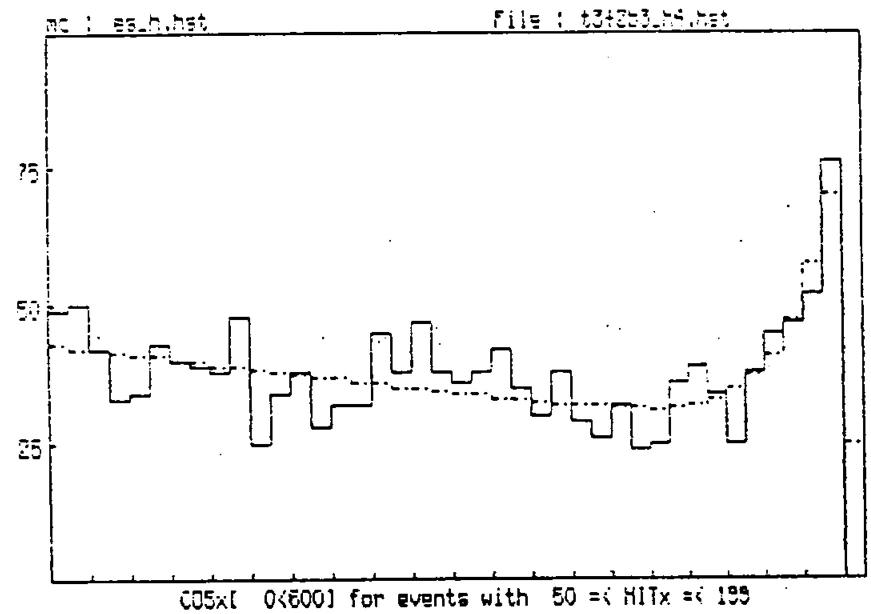

mc : es_h.hst
File : t3+2b3_h4.hst
75
50
25
CD5x[0<600] for events with 50 =< HITx =< 199

Figure 12

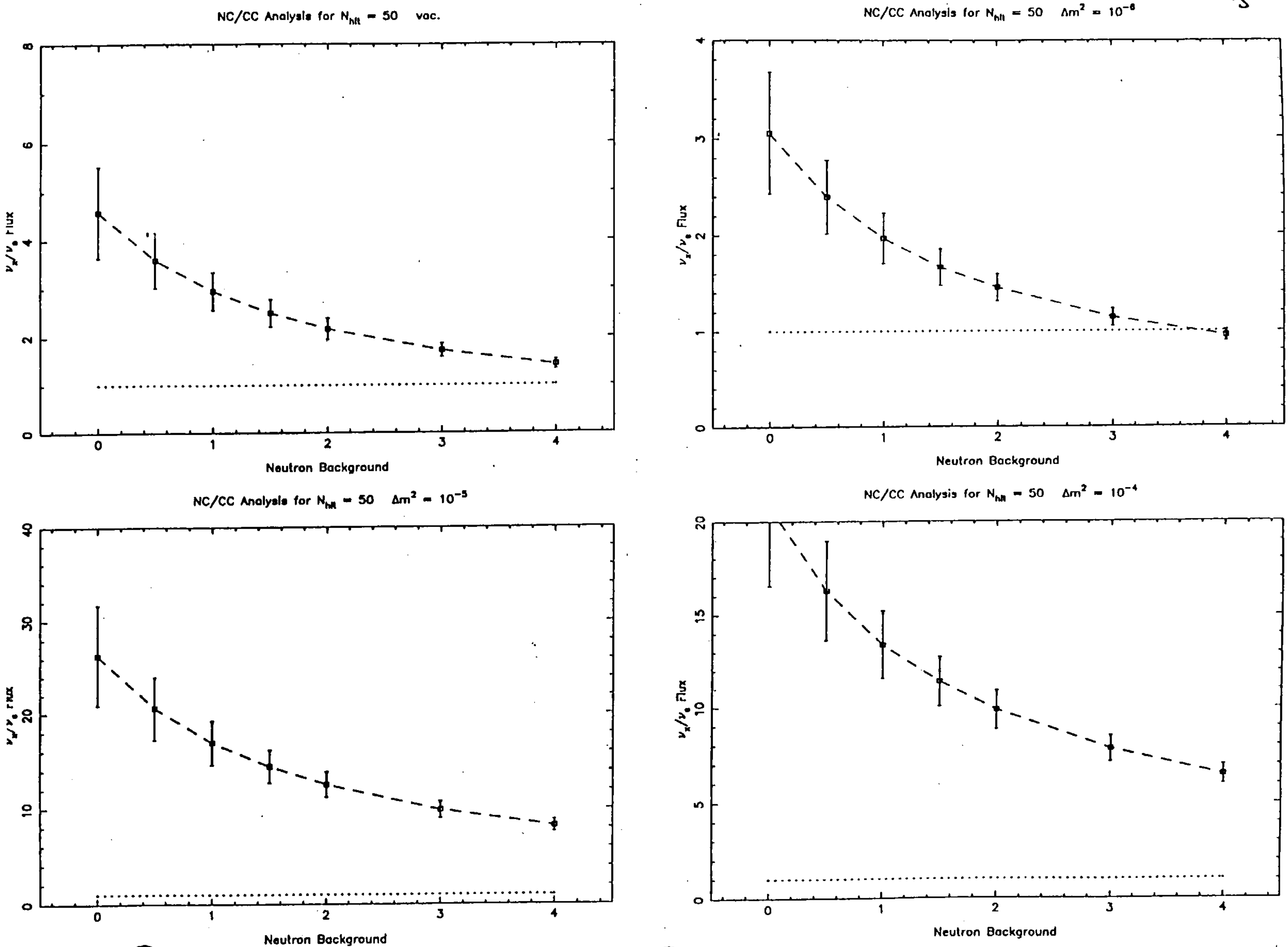

NC/CC Analysis for N_{hit} = 50 vac.
ν_x/ν_e Flux
Neutron Background
NC/CC Analysis for N_{hit} = 50 $\Delta m^2 = 10^{-6}$
ν_x/ν_e Flux
Neutron Background
NC/CC Analysis for N_{hit} = 50 $\Delta m^2 = 10^{-5}$
ν_x/ν_e Flux
Neutron Background
NC/CC Analysis for N_{hit} = 50 $\Delta m^2 = 10^{-4}$
ν_x/ν_e Flux
Neutron Background

Figure 13

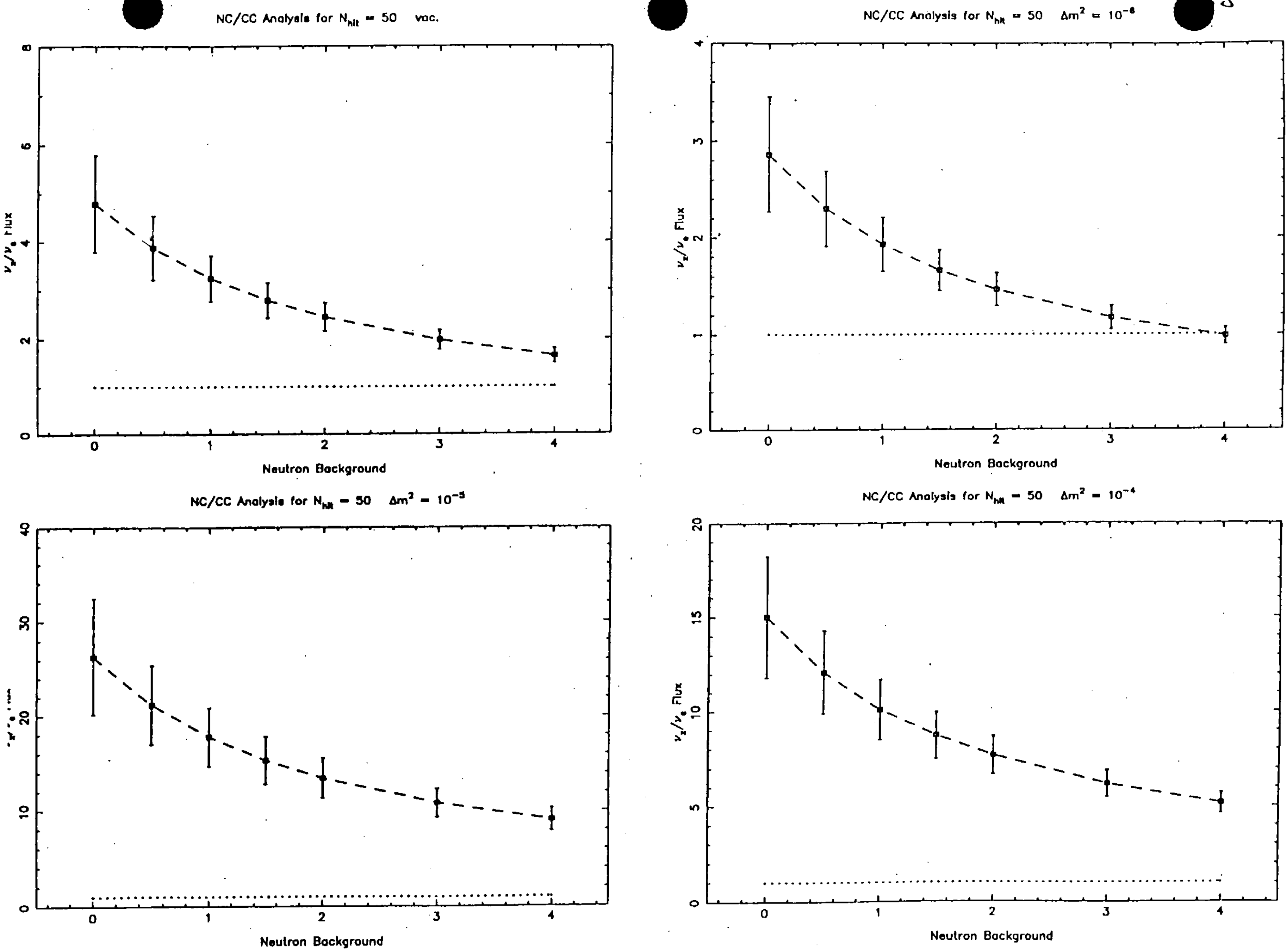

NC/CC Analysis for N_{hit} = 50 vac.
ν_x/ν_e Flux
Neutron Background
NC/CC Analysis for N_{hit} = 50 $\Delta m^2 = 10^{-6}$
ν_x/ν_e Flux
Neutron Background
NC/CC Analysis for N_{hit} = 50 $\Delta m^2 = 10^{-5}$
Neutron Background
NC/CC Analysis for N_{hit} = 50 $\Delta m^2 = 10^{-4}$
ν_x/ν_e Flux
Neutron Background